

## RADIATION EFFECTS IN GaAs AMOS SOLAR CELLS\*

B. K. Shin and R. J. Stirn  
Jet Propulsion Laboratory

### ABSTRACT

Inasmuch as GaAs solar cells show considerable potential for space applications, the behavior of these cells in a radiation environment is of great interest. This report presents the results of radiation damage produced in AMOS (Antireflecting-Metal-Oxide-Semiconductor) cells with  $\text{Sb}_2\text{O}_3$  interfacial oxide layers by 1-MeV electrons. The degradation properties of the cells as a function of irradiation fluences were correlated with the changes in their spectral response, C-V, dark forward, and light I-V characteristics. The active n-type GaAs layers were grown by the OM-CVD technique, using sulfur doping in the range between  $3 \times 10^{15}$  and  $7 \times 10^{16} \text{ cm}^{-3}$ . At a fluence of  $10^{16} \text{ e/cm}^2$ , the low-doped samples showed  $I_{\text{SC}}$  degradation of 8% and  $V_{\text{OC}}$  degradation of 8%. The high-doped samples showed  $I_{\text{SC}}$  and  $V_{\text{OC}}$  degradation of 32% and 1%, respectively, while the fill factor remained relatively unchanged for both. AMOS cells with water vapor-grown interfacial layers showed no significant change in  $V_{\text{OC}}$ .

### INTRODUCTION

Results of 1-MeV electron damage in n-base heteroface Al(Ga)As/GaAs solar cells are relatively sparse (ref. 1). More importantly, the results to date are primarily for base carrier concentrations in the low  $10^{17} \text{ cm}^{-3}$  regime. Also, since the photovoltaic parameters of the solar cell are affected by the Al(Ga)As layer thickness and depth of the junction, it has not been possible to separate damage effects occurring in the p- and n-regions of the cell. On the other hand, the wider body of literature of electron damage in bulk n-GaAs (refs. 2,3) usually measured only majority carrier removal or trap properties, such as by DLTS (Deep Level Trap Spectroscopy), and not the more important (for solar cells) changes in photovoltaic parameters or minority carrier lifetimes upon irradiation.

This paper presents preliminary results of radiation damage in GaAs introduced by 1-MeV electrons using Schottky barrier structures. This approach has the distinct advantage of being able to use GaAs with carrier concentrations

---

\* This paper presents the results of one phase of research conducted at the Jet Propulsion Laboratory, California Institute of Technology, for the Department of Energy by agreement with the National Aeronautics and Space Administration.

much less than  $10^{17} \text{ cm}^{-3}$  and observing degradation characteristics of GaAs Schottky barrier solar cells as developed at JPL. Since these are majority carrier devices, i.e., the voltage output and fill factor are not controlled by minority carrier diffusion from the bulk, reduced radiation damage should be observed as compared to junction type p/n solar cells. A disadvantage of using Schottky structures is that annealing studies of radiation damage are not possible since the devices are unstable at temperatures above  $200^\circ\text{C}$ .

The addition of an intentional interfacial oxide layer between the Schottky barrier metal and the GaAs has been found to dramatically increase the open circuit voltage  $V_{OC}$  from about 500 to 800 mV (ref. 4). Consequently, the irradiation studies of Schottky barrier solar cells were performed on devices incorporating two types of oxide layers to determine if electron irradiation will influence the  $V_{OC}$  by modifying the interface states controlling the Schottky barrier height.

#### EXPERIMENTAL DETAILS

The solar cells used in the present investigation were prepared by growing n-type GaAs epilayers by organo-metallic chemical vapor deposition (OM-CVD) techniques on Te-doped substrates and fabricating AMOS (Anti-reflecting Metal-Oxide-Semiconductor) solar cells on this material. The substrates\* had doping concentrations of  $2.7 \times 10^{17} \text{ cm}^{-3}$  and crystal orientation approximately  $2^\circ$ -off [100] toward the [110] direction. The active epilayer was sulfur-doped with the doping concentrations ranging from  $3 \times 10^{15}$  to  $7 \times 10^{16} \text{ cm}^{-3}$ . The epilayers of 3 to  $4 \mu\text{m}$  in thickness were grown at  $700^\circ\text{C}$  using arsine ( $\text{AsH}_3$ ) and trimethyl-gallium (TMG) flow rates of  $1.9 \times 10^{-4}$  and  $4.5 \times 10^{-5}$  moles/min, respectively. These epilayers were used to fabricate fully gridded and AR-coated  $1 \times 1$ -cm AMOS cells. No attempt was made to optimize the design parameters to increase radiation hardness.

Prior to cell fabrication, ohmic back contacts were made by sintering Au-Ge-Ni evaporated contacts for 3 min in hydrogen at  $480^\circ\text{C}$ . The interfacial oxide layers of the AMOS cells were formed using either vacuum-deposited  $\text{Sb}_2\text{O}_3$  oxides or saturated water vapor ( $\text{H}_2\text{O}/\text{O}_2$ ) native oxides. The non-native  $\text{Sb}_2\text{O}_3$  oxides of 38 Å thickness were deposited at a rate of 0.6 Å/sec in an oil-free vacuum chamber. The  $\text{H}_2\text{O}/\text{O}_2$ -generated oxides were formed at  $23^\circ\text{C}$  by passing water-vapor-saturated  $\text{O}_2$  over freshly etched GaAs placed in a quartz tube. Typical oxide formation time of 48 to 72 hours is required to obtain uniform oxide layers of 38 Å in the later case. A 60 Å-thick Ag layer of  $1\text{-cm}^2$  area was next evaporated at a typical rate of 5 Å/sec to form the Schottky barrier.

The 1-MeV electron irradiation was performed at JPL using the Dynamitron Particle Accelerator with fluences between  $10^{14}$  and  $10^{16} \text{ e/cm}^2$ . The irradiation was carried out at room temperature using an electron flux of  $\leq 10^{12} \text{ e/cm}^2\text{-sec}$ .

---

\*Epidyne (now National Semiconductor, Hawthorne, CA)

Properties of cells as a function of irradiation fluences were evaluated by the light current-voltage (I-V) characteristics, spectral response measurements, capacitance-voltage (C-V) and dark forward I-V characteristics. Light I-V measurements were obtained with samples at 28°C by using either the ELH lamps at input power density of 100 mW/cm<sup>2</sup> for AMI simulation or the Aerospace Controls Model 302 xenon arc source at an input power density of 135 mW/cm<sup>2</sup> for AMO simulation. Absolute spectral response measurements were made in the wavelength ranges between 0.4μm and 0.9μm using a prism monochromator. The output current of a standard Si PIN diode previously calibrated with a UDT 21A Power Meter was used to obtain absolute values of the collection efficiency.

The diodes were further evaluated using measurements of C-V and dark forward I-V characteristics in a light-tight box. The measurements of capacitance as a function of reverse voltage were obtained with a Boonton 74C-S8 Capacitance Bridge operating at 100 kHz.

## RESULTS AND DISCUSSION

Light I-V characteristics for two Sb<sub>2</sub>O<sub>3</sub>-oxide AMOS solar cells using ELH light simulation with carrier concentrations representing the extremes of those used in this study are given in figure 1 for pre-irradiated and post-irradiated conditions. The Sb<sub>2</sub>O<sub>3</sub>-oxide cells used in this study did not have permanent contacts applied, and thus, could not be measured in-situ with the AMO simulator. Solar cells with native oxides did have such contacts, but unfortunately did not include GaAs layers with concentrations below 1x10<sup>16</sup> cm<sup>-3</sup>.

Note that the lower-doped sample showed considerably less degradation in short-circuit current (I<sub>SC</sub>). This is because the space charge region width in low-doped GaAs is a significant fraction of the light-absorption depth, and photo-generated carriers in this region which are field-aided in their collection are little affected by radiation-induced defects. A second contributing factor to the lower degradation in more lightly-doped GaAs is probably a lower degradation constant related to minority carriers collected at the barrier by diffusion from the neutral region -- just as for silicon.

There is some degradation in V<sub>OC</sub> for these cells -- more for the lighter-doped GaAs. Though the amount of degradation at 10<sup>16</sup> e/cm<sup>2</sup> fluence, for example, is much less than usually observed in p/n junction-type solar cells, it is clearly more than that found for AMOS solar cells using H<sub>2</sub>O/O<sub>2</sub> native oxides, as shown in figure 2. This figure shows the V<sub>OC</sub> normalized to the pre-irradiated value as a function of fluence for several samples of various doping concentrations with both the native and the deposited interlayer oxides. Two features are clearly observed from these curves: (1) The overall degradation of V<sub>OC</sub> is not of major significance, since at a fluence of 10<sup>16</sup> e/cm<sup>2</sup>, the degraded values range from 2 to 8%, and (2) the degradation characteristics of the two types of oxides, the H<sub>2</sub>O/O<sub>2</sub> or the Sb<sub>2</sub>O<sub>3</sub> oxides, are quite distinguishable. In particular, the native oxide cells show negligible change, consistent with earlier unpublished results obtained at JPL on Te-doped GaAs layers. The small change is to be expected since the AMOS cell is a majority carrier device, as mentioned above.

To supplement the results for  $V_{OC}$ , the dark forward I-V characteristics were measured and the values of both the saturation current density  $J_0$  and the diode ideality factor  $n$  obtained using the least square fitting. The plots of  $J_0$  and  $n$  as a function of fluence are shown in figures 3 and 4, respectively. Samples with both types of oxide ( $H_2O/O_2$  and  $Sb_2O_3$ ) interlayers are shown for comparison. The differences in  $J_0$  (and  $n$ ) between samples relate more to differences in surface treatment and handling immediately prior to oxidation rather than to differences in doping or even oxide type. The values of  $J_0$  and  $n$  do not change much with increasing fluence except at fluences higher than  $10^{15}$  e/cm<sup>2</sup>, with more change seen in the  $Sb_2O_3$ -oxide solar cells.  $J_0$  and the  $n$ -factor are intimately related to each other in Schottky barriers with interfacial oxide layers.

The effects of electron irradiation on the short-circuit current for cells with various doping concentrations are shown in figure 5. As expected, the degradation is more pronounced in  $I_{SC}$  than in  $V_{OC}$ . The results for a LPE-grown Al(Ga)As-GaAs heteroface solar cell (ref. 1) with junction depth of  $0.5\mu m$  and the donor doping of  $10^{17}$  cm<sup>-3</sup> is also included for comparison. Clearly, the percentage change in  $I_{SC}$  per given fluence primarily depends on the doping concentrations and is independent of the type of oxide used. This is typical of the Schottky barrier cells, with relatively high doping, where the degradation of  $I_{SC}$  is primarily due to a decrease in diffusion length as for Si solar cells. More specifically, the change in  $I_{SC}$  is directly related to the ratio of light-generated carrier density in the depletion region to that in the bulk. Finally, the anomalous behavior of  $10^{16}$  cm<sup>-3</sup> doped cells is noteworthy for fluence between  $10^{15}$  and  $10^{16}$  e/cm<sup>2</sup>. This reverse degradation reproducibly occurred for several samples tested with the same doping level. To our knowledge, such irregularity has not been reported in the literature, although GaAs solar cells with doping concentrations of  $10^{16}$  cm<sup>-3</sup> are rarely made. Further experiments on this matter are planned.

Figure 6 shows the absolute collection efficiency as a function of wavelength from  $0.4\mu m$  to the bandgap region, for both unirradiated and  $10^{16}$  e/cm<sup>2</sup> irradiated cells having various bulk concentrations. The spectral response is consistent with the behavior of the short-circuit current, in that the red region is more affected for the highly-doped cell. The zero-bias depletion width of the lightly doped cells is large ( $\sim 0.7\mu m$  for  $n_0 = 3 \times 10^{15}$  cm<sup>-3</sup>) before the irradiation, increasing with fluence because of carrier removal. Since the absorption depths for  $\lambda = 0.7\mu m$  and  $0.5\mu m$  is  $0.65\mu m$  and  $0.1\mu m$ , respectively, it is clear that most of the incident energy will be absorbed within the depletion width for the lower-doped cells.

The dependence of fill factor (FF) as a function of fluence for four  $H_2O/O_2$  samples is shown in figure 7. Averaged FF values were used since the values at each fluence level were very similar for all of the samples evaluated. At the highest fluence level, the spread of FF is only  $\pm 0.2\%$  from the average value. The unirradiated FF of 0.79 is reasonably good and gradually decreases to 0.73 at  $6.25 \times 10^{15}$  e/cm<sup>2</sup> -- a decrease of less than 8%. The small change of FF in Schottky barrier devices is due to the relatively small change in  $J_0$  with fluence, as compared to junction-type solar cells.

Power degradation for the  $H_2O/O_2$  cells with doping concentrations of  $1 \times 10^{16}$  and  $5 \times 10^{16} \text{ cm}^{-3}$  is shown in figure 8. A typical degradation characteristic for a heteroface cell with Al(Ga)As/GaAs structure grown by LPE is also included for comparison. In the  $H_2O/O_2$  AMOS cells, about 24% degradation is obtained for lower-doped cell ( $n_0 = 1 \times 10^{16} \text{ cm}^{-3}$ ) at  $10^{16} \text{ e/cm}^2$ . Even lower power degradation (17%) was observed on the  $3 \times 10^{15} \text{ cm}^{-3}$  cells having  $Sb_2O_3$  oxide interlayer when measured with ELH simulation. However, due to absence of contacts, no in-situ AMO values are given. Note the anomalous behavior of the  $10^{16} \text{ cm}^{-3}$  sample due to the aforementioned behavior in  $I_{SC}$  (fig. 5).

When the carrier concentration is plotted against a critical fluence at which  $I_{SC}$  degrades by the same amount, e.g. 25%, (fig. 9), an apparent break in the slope occurs at the same carrier concentration at which the  $I_{SC}$  degradation was observed ( $10^{16} \text{ cm}^{-3}$ ). For this figure, data was taken from an earlier study, not previously reported, where the GaAs epi-layers were commercially purchased Te-doped layers. At this time, it is not clear whether an abrupt change in slope is indeed real, or if the two slopes are indicative of two very separate mechanisms. Thus, the critical fluence should tend to become independent of doping in the light-doping range, where substantially all of the carriers are generated in the space-charge region. At higher doping levels, where substantially all of the carriers must diffuse from the neutral region of the bulk GaAs, one would expect a constant dependence of the critical fluence on carrier concentration. A determination of the detailed mechanisms will require additional studies and will be reported subsequently.

#### REFERENCES

1. "High Efficiency GaAs Solar Cell" Final Report, January 1979, AFAPL-TR-78-96, Hughes Aircraft Company.
2. D. V. Lang, R. A. Logan, and L. C. Kimerling, Phys. Rev. B15, 4874 (1977).
3. J. W. Farmer and D. C. Look, submitted to Physical Review.
4. R. J. Stirn and Y. C. M. Yeh, IEEE Trans. Electron Dev. ED-24, 476 (1977).

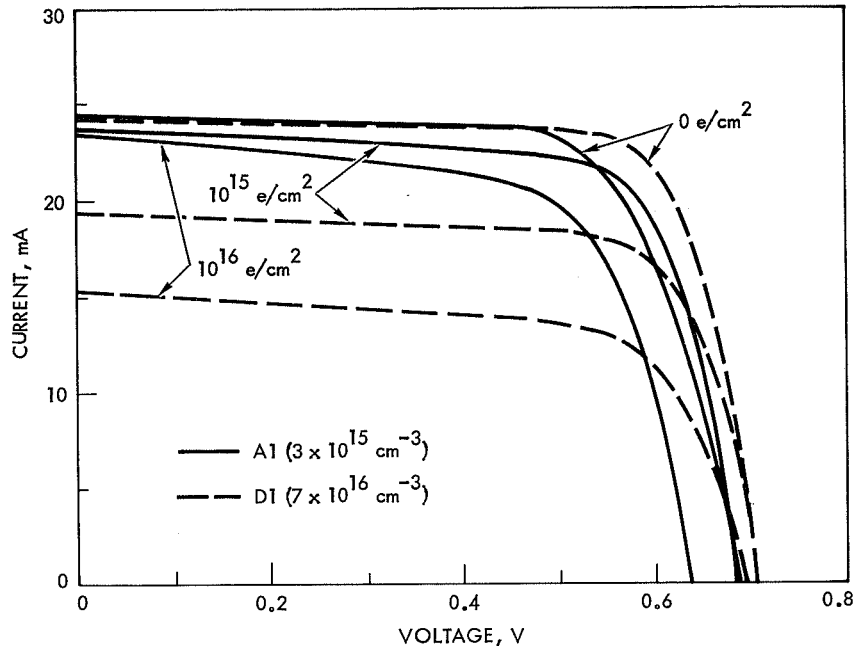


Figure 1. Light I-V Characteristics of Non-Irradiated and 1-MeV Electron-Irradiated GaAs AMOS Solar Cells With  $Sb_2O_3$ -Oxide Interlayer

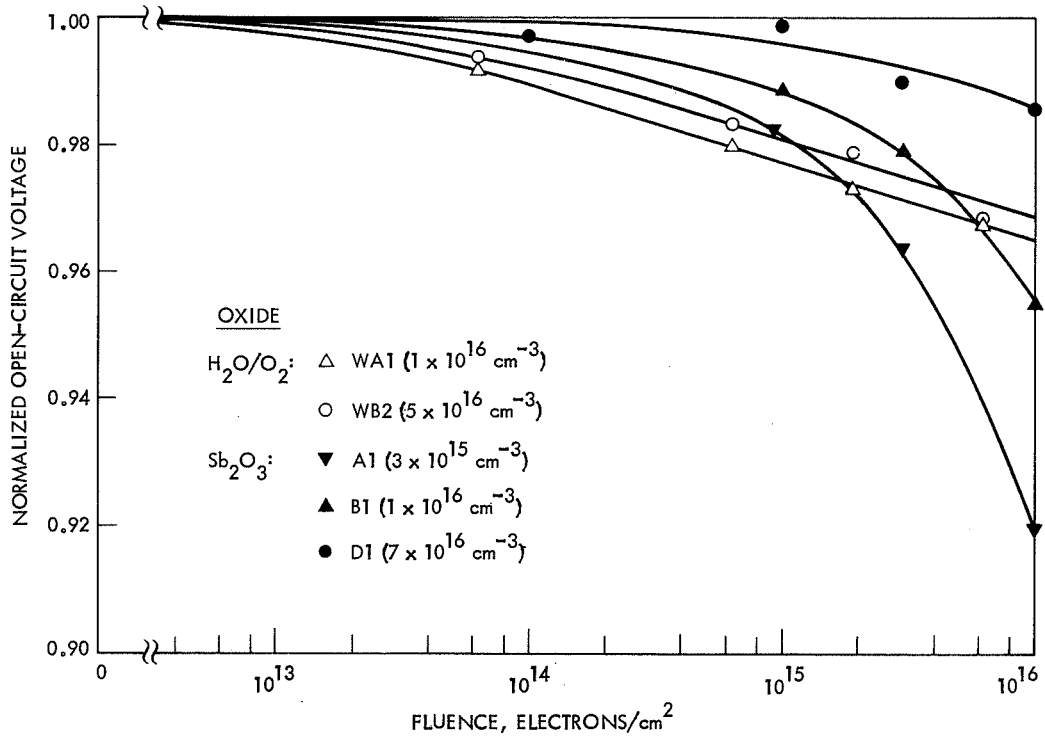


Figure 2. Normalized Open-Circuit Voltage as a Function of Fluence for GaAs AMOS Solar Cells Irradiated with 1-MeV Electrons

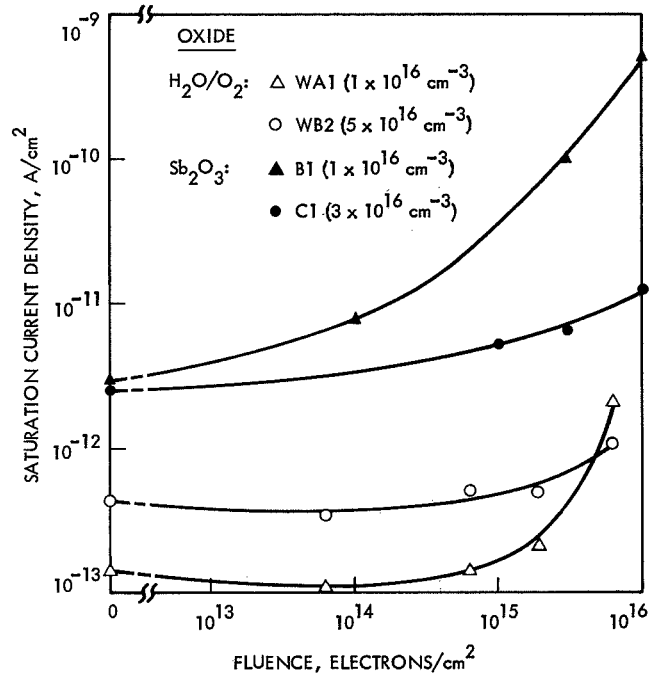


Figure 3. Saturation Current Density as a Function of Fluence for GaAs AMOS Solar Cells Irradiated with 1-MeV Electrons

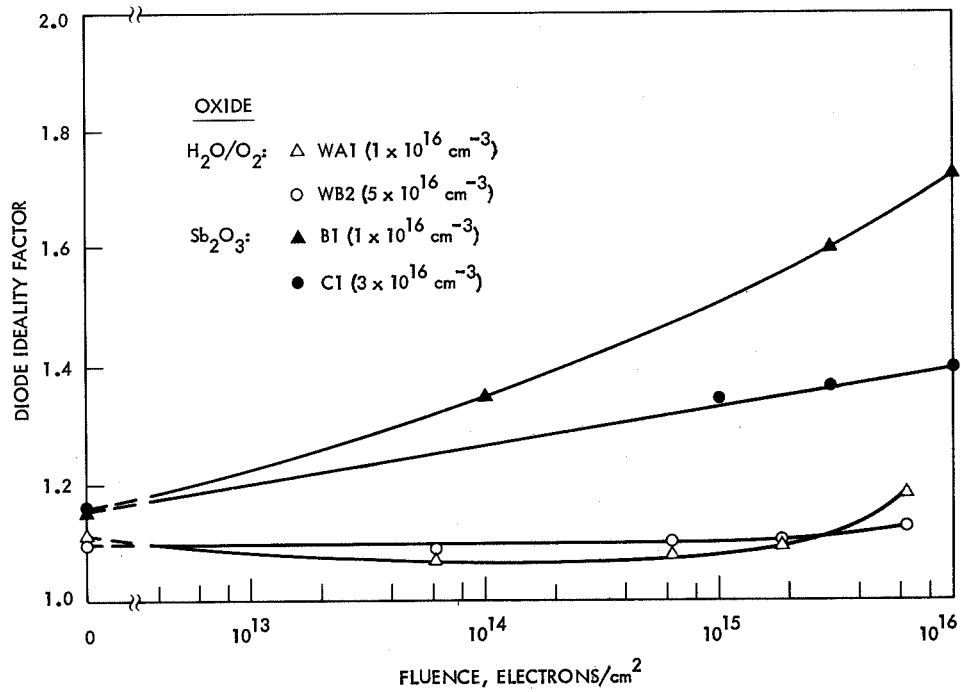


Figure 4. Diode Ideality Factor as a Function of Fluence for GaAs AMOS Solar Cells Irradiated with 1-MeV Electrons

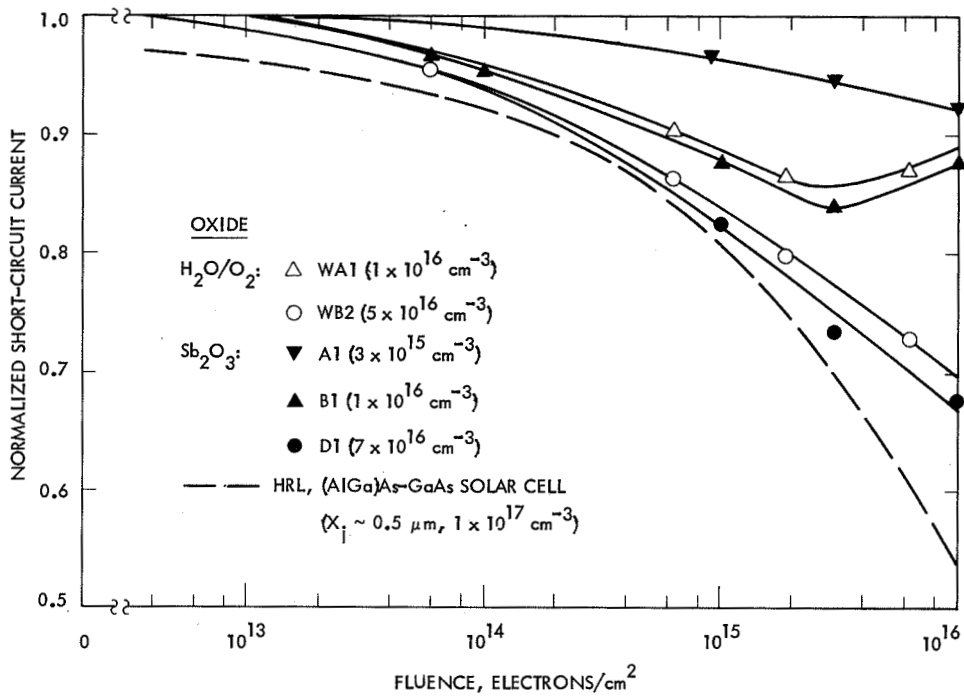


Figure 5. Normalized Short-Circuit Current as a Function of Fluence for GaAs AMOS Solar Cells Irradiated with 1-MeV Electrons

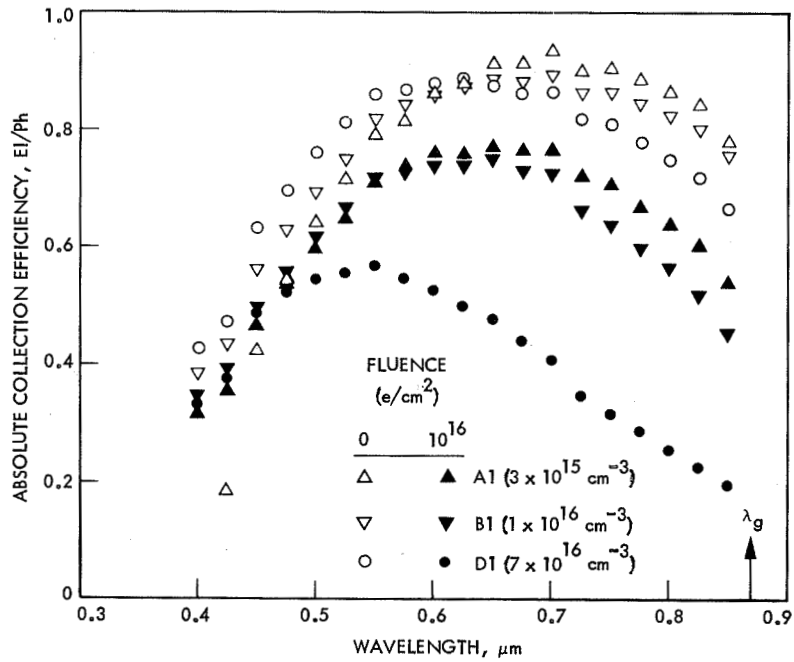


Figure 6. Absolute Spectral Response of GaAs AMOS Solar Cells Non-Irradiated and Irradiated with 1-MeV Electrons to 10<sup>16</sup> e/cm<sup>2</sup> Fluence



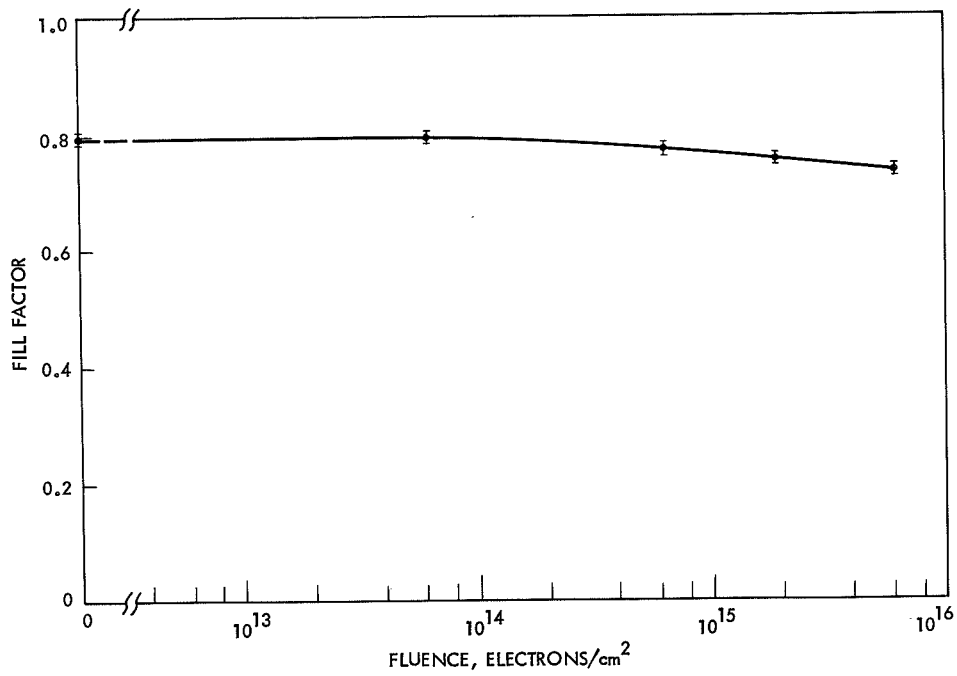


Figure 7. Fill Factor as a Function of Fluence for GaAs AMOS Solar Cells with  $H_2O/O_2$  Oxide Interlayers Irradiated with 1-MeV Electrons (Averaged for four samples)

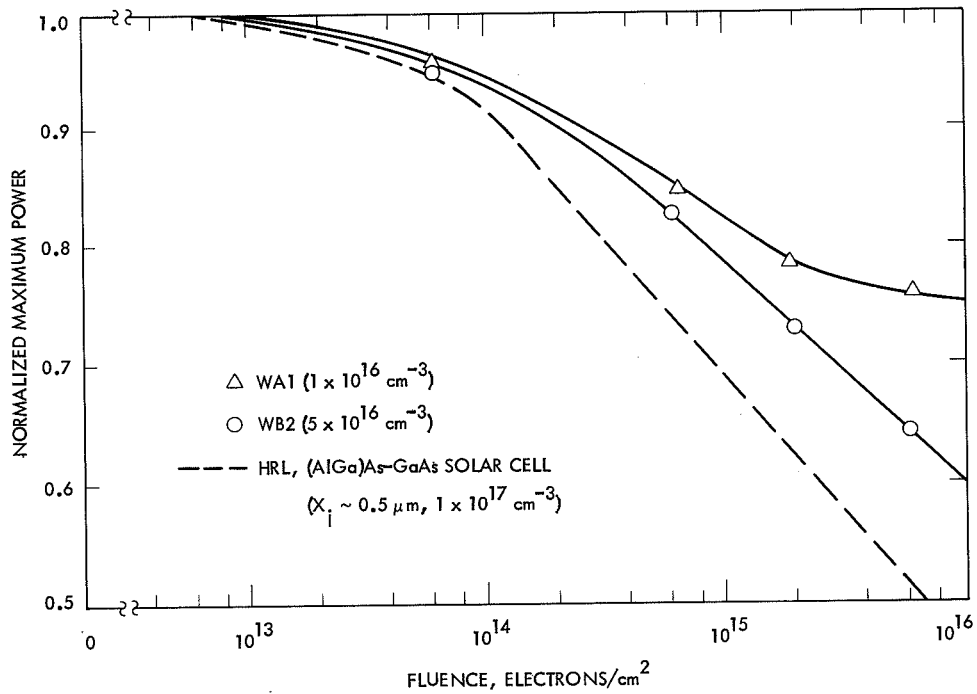


Figure 8. Normalized Maximum Power as a Function of Fluence for GaAs AMOS Solar Cells with  $H_2O/O_2$  Oxide Interlayer Irradiated with 1-MeV Electrons

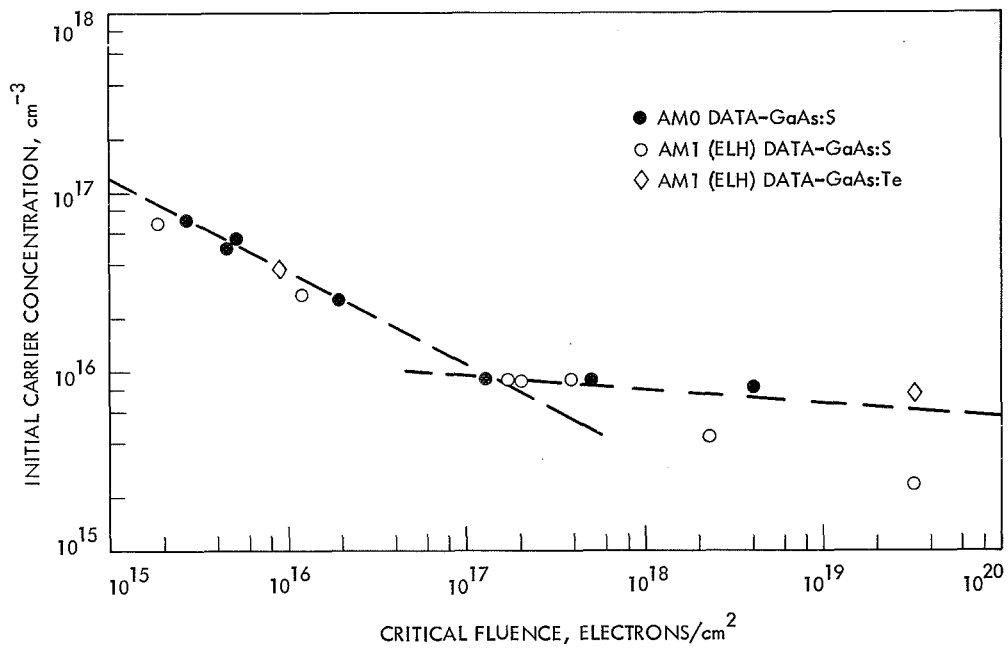


Figure 9. Initial (Non-Irradiated) Carrier Concentration of GaAs AMOS Solar Cells as a Function of Critical Fluence at which the Short-Circuit Current Degraded by 25% of the Unirradiated Value